Phytochemistry 138 (2017) 65–75

Contents lists available at ScienceDirect

Phytochemistry

journal homepage: www.elsevier.com/locate/phytochem

Isolation and characterization of *9-lipoxygenase* and *epoxide hydrolase 2* genes: Insight into lactone biosynthesis in mango fruit (*Mangifera indica* L.)

Ashish B. Deshpande [a], Hemangi G. Chidley [a], Pranjali S. Oak [a], Keshav H. Pujari [b], Ashok P. Giri [a], Vidya S. Gupta [a, *]

[a] Plant Molecular Biology Unit, Division of Biochemical Sciences, CSIR-National Chemical Laboratory, Pune, 411 008, India
[b] Dr. Balasaheb Sawant Konkan Agriculture University, Dapoli, 415712, India

ARTICLE INFO

Article history:
Received 20 December 2016
Received in revised form
3 March 2017
Accepted 5 March 2017
Available online 11 March 2017

Chemical compounds studied in this article:
Gamma-hexalactone (PubChem CID: 12756)
Delta-hexalactone (PubChem CID: 13204)
Delta-valerolactone (PubChem CID: 10953)
Delta-decalactone (PubChem CID: 12810)
12(13) EpOME (PubChem CID: 5356421)
9HpODE (PubChem CID: 9548877)
9HpOTrE (PubChem CID: 5282864)

Keywords:
Mangifera indica
Anacardiaceae
Lactone biosynthesis
Transient expression
9-Lipoxygenase
Epoxide hydrolase 2

ABSTRACT

Uniqueness and diversity of mango flavour across various cultivars are well known. Among various flavour metabolites lactones form an important class of aroma volatiles in certain mango varieties due to their ripening specific appearance and lower odour detection threshold. In spite of their biological and biochemical importance, lactone biosynthetic pathway in plants remains elusive. Present study encompasses quantitative real-time analysis of *9-lipoxygenase* (*Mi9LOX*), *epoxide hydrolase 2* (*MiEH2*), *peroxygenase*, *hydroperoxide lyase* and *acyl-CoA-oxidase* genes during various developmental and ripening stages in fruit of Alphonso, Pairi and Kent cultivars with high, low and no lactone content and explains their variable lactone content. Study also covers isolation, recombinant protein characterization and transient over-expression of *Mi9LOX* and *MiEH2* genes in mango fruits. Recombinant *Mi*9LOX utilized linoleic and linolenic acids, while *Mi*EH2 utilized aromatic and fatty acid epoxides as their respective substrates depicting their role in fatty acid metabolism. Significant increase in concentration of δ-valerolactone and δ-decalactone upon *Mi9LOX* over-expression and that of δ-valerolactone, γ-hexalactone and δ-hexalactone upon *MiEH2* over-expression further suggested probable involvement of these genes in lactone biosynthesis in mango.

1. Introduction

Acceptability and preference of food items is based on human organoleptic perception, which is a combined impression of visual appearance, texture, aroma and taste of a specific item. A collective olfaction of aroma and taste through retronasal and orthonasal receptors and taste buds decides flavour of the food. It is well known that aroma compounds mainly contribute to the flavour of the food. Most of the aroma related studies have been carried out on various fruits, as they possess unique aroma with large diversity in their respective flavour profile.

Aroma volatile analysis of *Mangifera indic*a L. (Anacardiaceae) has shown presence of various groups of volatile compounds *viz.* alkanes, alkenes, aldehydes, alcohols, monoterpenes, sesquiterpenes, oxygenated monoterpenes, oxygenated sesquiterpenes, non-terpene hydrocarbons, furanones and lactones (Dar et al., 2016; Idstein and Schreier, 1985; Pandit et al., 2009b). Alphonso, one of the most favoured and exported Indian mango cultivars has revealed qualitative abundance and blend of volatiles among the 22 Indian and 5 exotic mango cultivars analysed (Pandit et al., 2009a). Among these groups of volatile compounds lactones and furanones are notably important due to their ripening specific temporal and spatial appearance in mango fruits (Pandit et al., 2009b).

* Corresponding author.
E-mail address: vs.gupta@ncl.res.in (V.S. Gupta).

http://dx.doi.org/10.1016/j.phytochem.2017.03.002
0031-9422/

Interestingly 14 different lactones have been reported from Alphonso, which is the highest number of lactones known from any single fruit (Idstein and Schreier, 1985; Wilson et al., 1990). Structurally these lactones are cyclic esters characterized by a closed ring consisting of four or five carbon atoms and a single oxygen atom, with a ketone group (C=O) in one of the carbons adjacent to oxygen in the ring. These lactones, although present in very low concentration in analysed tissues (7–26 $\mu g g^{-1}$), pose high impact on overall flavour of Alphonso mango due to their lower odour detection threshold values (Kulkarni et al., 2012). They impart sweet fruity flavour, a characteristic feature of fully ripened mango fruit (Wilson et al., 1990). Thus, lactones can be considered as marker metabolites of Alphonso ripening. Despite the structural and functional characterization of these vital flavour metabolites, the pathway of their biosynthesis remains elusive.

Earlier attempts to identify probable precursors of lactone biosynthesis, even if in other organisms, can form a basis to reveal lactone biosynthesis in mango. For example, studies in various yeasts, moulds and bacteria suggest that fatty acids and keto acids might be the precursors at initial steps of lactone biosynthesis. The hydroxy fatty acids then synthesized (probably upon microbial reduction) from various γ and δ keto acids (C8–C12) could be converted into lactones by simple heating (Muys et al., 1962). Deuterium labelling studies in yeast (*Sporobolomyces odorus*) have revealed involvement of unsaturated fatty acids such as linolenic acid as precursors for δ-Jasmin lactone and (Z,Z)-Dodeca-6,9-dieno-4-lactone synthesis (Haffner et al., 1996). Metabolism of epoxy octadecanoic acid by epoxide hydrolase (EH) for production of γ-decalactone and γ-dodecalactone has also been proposed through deuterium labelling studies in *Sporidiobolus salmonicolor* (Haffner and Tressl, 1998). Further, a study in nectarines has illustrated that administration of ^{18}O labelled epoxy acid-5 (9–10 epoxy heptadecanoic acid) produced undecano-4-lactone. This important observation has suggested possible involvement of epoxy fatty acids in lactone production by the activity of EH (Schottler and Boland, 1996). Comparative EST analysis from ripening *Prunus persica* L. Batsch has later supported *EH* as the key gene responsible for lactone biosynthesis (Vecchietti et al., 2009). These epoxy fatty acids in plants are synthesized by the activity of peroxygenase (PGX) enzyme (Fuchs and Schwab, 2013; Meesapyodsuk and Qiu, 2011). A report in Oat PGX (*As*PGX1) revealed that it catalyzes epoxidation of oleic acid with the cumene hydroperoxide as an oxidant. Similarly, *As*PGX1 utilizes products of 9-lipoxygenase (9LOX) *viz.* 9-hydroperoxy-octadecadienoic (9-HOPD) and 9-hydroperoxy-octadecatrienoic (9-HOPT) acids as oxygen donor (Meesapyodsuk and Qiu, 2011) generating their respective monohydroxy fatty acids. Also, involvement of lipoxygenase (LOX) to form oxygenated chiral fatty acids leading to production of γ and δ lactones upon beta oxidation has also been reported (Cardillo et al., 1989). Also significance of hydroxy fatty acid synthesized from products of 9LOX i.e. hydroperoxy fatty acid in the formation of lactone is reported (Huang and Schwab, 2011).

These initial efforts insinuate involvement of LOX and EH enzymes in lactone biosynthesis. The present study focuses on isolation and transcript profiling of *9-lipoxygenase* (*Mi9LOX*), *epoxide hydrolase 2* (*MiEH2*), *peroxygenase* (*MiPGX1*), *hydroperoxide lyase* (*MiHPL*) and *acyl-CoA-oxidase* (*MiACO*) genes during various developmental and ripening stages in fruit of Alphonso, Pairi and Kent cultivars having differential levels of lactones. Further, molecular and biochemical characterization of *Mi9LOX* and *MiEH2* in mango fruit and probable role of these two enzymes in lactone biosynthesis have been investigated based on their over-expression by agroinfiltration approach followed by metabolite analysis.

2. Results

2.1. In silico analysis of isolated genes from Mangifera indica L.

EH from mango depicted ORF of 957 nucleotides with 74 and 241 nucleotides long 5′ and 3′ UTR regions, respectively. While in case of *LOX*, ORF of 2526 nucleotides with only 3' UTR (167 nucleotides) was evident. These mango genes showed similarity with linoleate *9-lipoxygenase* and soluble *EH2* reported from other plant species with maximum similarity with *Citrus sinensis* (80%) and *Prunus persica* (75%), respectively. Further phylogenetic analysis of encoded protein sequences of *LOX* and *EH* genes in our study along with the other plant 9LOX, 13LOX, EH1 and EH2 sequences reported in the NCBI database showed four distinct clusters in cladogram each representing 9LOX, 13LOX, EH1 and EH2, respectively (Fig. 1); wherein mango LOX and EH grouped in clads of other plant 9LOX and EH2, respectively. Hence these were named as *Mi9LOX* (KX090178) and *MiEH2* (KX090179), respectively.

The other three genes from mango, *viz. MiPGX1* (KX090180), *MiHPL* (KX090181) *and MiACO* (KX090182) upon *in silico* analysis showed presence of complete ORF's of 708, 1485 and 1995 bp, respectively. Sequence analysis of respective genes confirmed their maximum similarities with reported sequences of *peroxygenase* (80%), *hydroperoxide lyase* (76%) and *acyl-CoA-oxidase* (86%) from *Citrus sinensis*.

2.2. Expression of Mi9LOX, MiHPL, MiPGX1, MiEH2 and MiACO in fruits of three mango cultivars

Transcript abundance of five candidate genes, *viz. Mi9LOX, MiHPL, MiPGX1, MiEH2* and *MiACO* was studied in pulp and skin tissues of fruit of Alphonso, Pairi and Kent cultivars at various stages of fruit development and ripening. Transcript levels of the individual genes from three cultivars at their maxima were not significantly different; however their differential expression was evinced at various ripening stages and in pulp and skin tissues of the three cultivars. Transcript level of each gene at its maximum expression was considered as 1 and its relative expression in pulp and skin of various stages was represented across cultivars (Figs. 2 and 3). All the three cultivars showed ripening specific appearance of *Mi9LOX*, *MiPGX1* and *MiACO* transcripts (Figs. 2 and 3). Relative quantification of *MiPGX1* showed optimum transcripts at mid ripe stage in the pulp as well as the skin tissues of Alphonso and Pairi cultivars, which later reduced significantly till over ripe stage. Whereas, *MiPGX1* transcript level in the pulp and the skin tissues of Kent cultivar increased continuously from table green stage to over ripe stage. *MiPGX1* transcript abundance from the skin tissue of Kent was very low compared to that in the pulp tissue. However, *MiPGX1* expression level was almost similar in the case of pulp and skin tissues of Pairi and 25% low in the case of Alphonso pulp than the skin tissue. *MiEH2* transcripts in Alphonso were found to be the highest during mature raw and table green stages of the pulp and skin tissues. These levels were almost 50% lower in the skin tissue as compared to the pulp. In case of Pairi *MiEH2* transcripts were optimum at mature raw stage of the pulp tissue, which reduced by 60% at 60 DAP stage of the skin compared to the pulp. Interestingly, the pulp and the skin tissues of Kent showed expression of *MiEH2* throughout the developing and ripening stages. *MiHPL* transcripts were abundant in the developing tissues of Alphonso and Pairi, which further reduced to nearing zero at post table green stage. In case of Kent *MiHPL* transcripts were present throughout the developing and the ripening stages of the pulp and the skin tissues. Relative transcript profiles of *Mi9LOX* and *MiACO* from Alphonso pulp revealed their high abundance through mid ripe stage to over ripe stage, whereas, slight reduction in their level was observed at

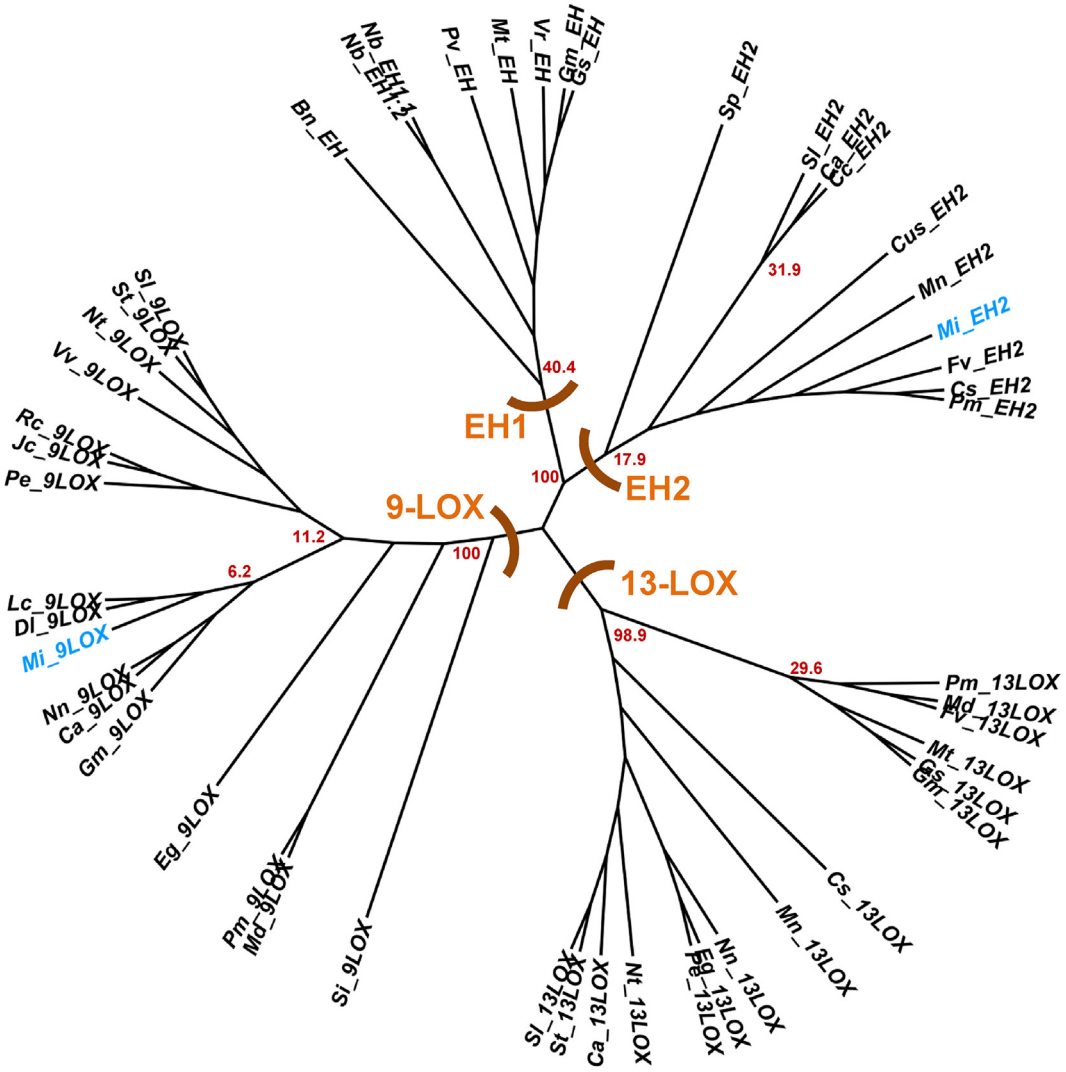

Fig. 1. Cladogram representing phylogenetic analysis by neighbor-joining of encoded proteins by *Mi9LOX* and *MiEH2* (blue colour) genes with that of other plant 9LOX, 13LOX, EH1 and EH2 sequences. Node label represents name of the enzyme followed by two letters representing initials of botanical name of the plant. The numbers (red colour) at the branch nodes signify the bootstrap scores acquired after 1000 trials. Details of sequence of plant species, enzyme and NCBI accession in parenthesis are as follows; *Nicotiana benthamiana*_EH1.2 (ACE82566), *Nicotiana benthamiana*_EH1.1 (ACE82565), *Phaseolus vulgaris*_EH (AKJ75509), *Glycine max*_EH (CAA55294), *Medicago truncatula*_EH (XP_003626202), *Glycine soja*_EH (KHN43314), *Vigna radiata*_EH (AIJ27456), *Brassica napus*_EH (NP_001302895), *Citrus sinensis*_EH2 (XP_006489040), *Prunus mume*_EH2 (XP_016647751), *Cicer arietinum*_EH2 (XP_004508197), *Fragaria vesca*_EH2 (XP_004290776), *Cajanus cajan*_EH2 (KYP58120), *Cucumis sativus*_EH2 (XP_004134492), *Solanum lycopersicum*_EH2 (XP_004252913), *Solanum pennellii*_EH2 (XP_015077274), *Morus notabilis*_EH2 (XP_010105136), *Vitis vinifera*_9LOX (XP_010659859), *Malus domestica*_9LOX (NP_001281030), *Prunus mume*_9LOX (XP_008246456), *Glycine max*_9LOX (XP_003521704), *Solanum tuberosum*_9LOX (NP_001274916), *Nicotiana tabacum*_9LOX (XP_016433823), *Dimocarpus longan*_9LOX (ANF89411), *Corylus avellana*_9LOX (CAD10740), *Litchi chinensis*_9LOX (AEQ30071), *Populus euphratica*_9LOX (XP_011023610), *Eucalyptus grandis*_9LOX (XP_010025195), *Jatropha* curcas_9LOX (XP_012089053), *Ricinus communis*_9LOX (XP_002512386), *Solanum lycopersicum*_9LOX (XP_004244890), *Sesamum indicum*_9LOX (XP_011087404), *Nelumbo nucifera*_9LOX (XP_010256003), *Malus domestica*_13LOX (NP_001280985), *Prunus mume*_13LOX (XP_008228181), *Medicago truncatula*_13LOX (XP_003627308), *Solanum tuberosum*_13LOX (NP_001275115), *Glycine soja*_13LOX (KHN39622), *Fragaria vesca*_13LOX (XP_004303702), *Morus notabilis*_13LOX (XP_010086794), *Eucalyptus grandis*_13LOX (XP_010033729), *Populus euphratica*_13LOX (XP_011035732), *Nelumbo nucifera*_13LOX (XP_010273845), *Capsicum annuum*_13LOX (NP_001311748), *Nicotiana tabacum*_13LOX (XP_016495606), *Citrus sinensis*_13LOX (XP_006465905), *Solanum lycopersicum*_13LOX (AAB65767), *Glycine max*_13LOX (XP_014624448). (For interpretation of the references to colour in this figure legend, the reader is referred to the web version of this article.)

post mid ripe stage in case of the skin tissue. *Mi9LOX* and *MiACO* transcripts from Pairi pulp and skin tissues showed their maximum level at table green stage except for optimum level for *Mi9LOX* at mid ripe stage of Pairi pulp. Reduction in the *Mi9LOX* and *MiACO* level was evinced in further ripening stages of Pairi tissues. In the case of Kent pulp, *Mi9LOX* and *MiACO* transcript abundance was the highest at ripe stage, whereas in case of Kent skin tissue transcript level was higher at over ripe stage. Interestingly, co-expression of *MiPGX1*and *MiEH2* was observed for short duration in Alphonso fruits from table green stage to ripe stage (10 days) and in Pairi fruits from mature raw stage to ripe stage (8 days). While in case of Kent fruits co-expression of *MiPGX1* and *MiEH2* was noted throughout the ripening stages.

2.3. Heterologous expression and catalytic activities of proteins encoded by Mi9LOX and MiEH2

The *Mi9LOX* gene from Alphonso mango encoded protein of 841 aa with calculated molecular weight of ~96.3 kDa and 78% similarity with 9LOX of *Litchi chinensis*. Presence of conserved substrate binding and oxygen binding domains (Santino et al., 2005) were also revealed when the amino acid sequence alignment and

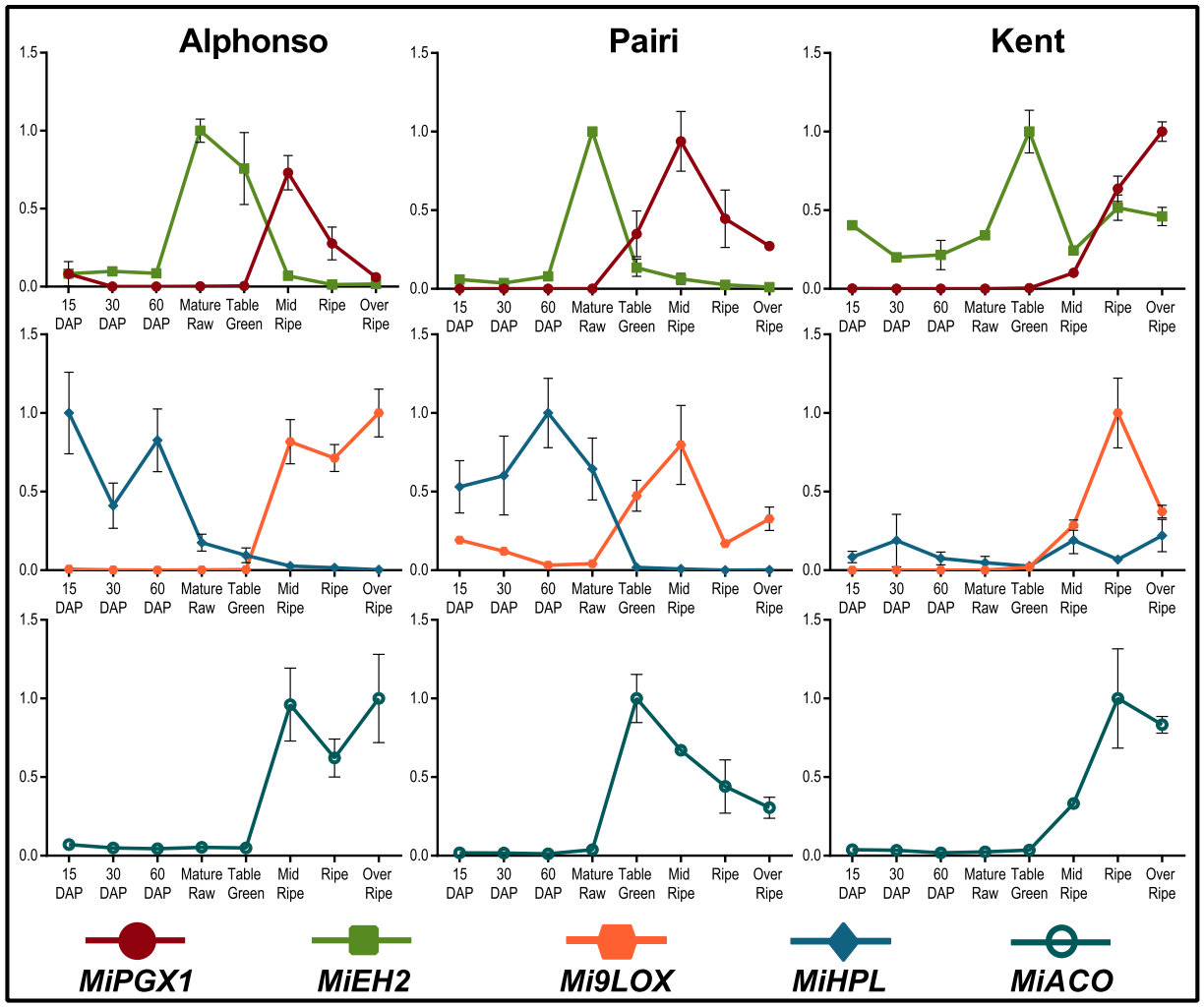

Fig. 2. Transcript profiles of *Mi9LOX*, *MiHPL*, *MiPGX1*, *MiEH2* and *MiACO* from pulp tissue of various fruit development and ripening stages of Alphonso, Pairi and Kent mango cultivars. Vertical bars at each data point represent standard error in the relative quantification among the biological replicates. X axis represents fruit development and ripening stages and Y axis represents relative transcript abundance.

secondary structure prediction of *Mi*9LOX was performed with that of *Glycin max* (PDB- 2iuj), *Vitis vinifera*, *Solanum lycopersicum* and *Litchi chinensis* using ESpript 3.0 software (Supplementary Fig. SF1). *MiEH2* from Alphonso mango encoded 318 aa long protein with calculated molecular weight of ~35.9 kDa and 81% similarity with predicted bifunctional epoxide hydrolase 2 from *Citrus sinensis*. Further secondary structure prediction and alignment of *Mi*EH2 with epoxide hydrolases from other plants, *viz*. *Solanum tuberosum* (PDB-2cjp), *Citrus sinensis* and *Nicotiana benthamiana* showed conserved catalytic residues (Supplementary Fig. SF2) (Bellevik et al., 2002b).

The encoded protein sequences of *Mi*9LOX and *Mi*EH2 were also analysed on **PRO**tein **SO**lubility evaluator (PROSO) to understand solubility of the expressed recombinant proteins. Both, *Mi*9LOX and *Mi*EH2 belonged to the solubility class with probability of 0.696 and 0.506, respectively. SDS-PAGE analysis indicated recombinant *Mi*EH2 protein purity to be good (Fig. 4a) to carry out enzymatic activity studies, whereas *Mi*9LOX eluted fractions had low molecular weight nonspecific proteins, which were eliminated by further purification step (Fig. 4b and c).

The enzymatic activity of purified recombinant *Mi*9LOX using linoleic acid (LA) and linolenic acid (ALA) as substrates revealed formation of 9HpODE and 9HpOTrE products, respectively (Supplementary Fig. SF3). Biochemical characterization of *Mi*9LOX revealed considerably high activity between pH 6 to 8 with optima at pH 6.5 and over 40% reduction in the activity at pH 5 and 9 (Supplementary Fig. SF4). Activity profile of *Mi*9LOX at varied temperatures showed stable activity of the enzyme between 37 and 45 °C, with temperature optima at 37.0 °C (Table 1) while 75 and 69% reduction in the activity at 35 and 50 °C, respectively. The enzyme kinetics for *Mi*9LOX with LA and ALA revealed more affinity towards ALA than LA based on the calculated Km values (Table 1) from *in vitro* studies. Similarly, Vmax/Km values of recombinant *Mi*9LOX showed higher catalytic efficiency with ALA than LA (Table 1).

Purified recombinant *Mi*EH2 showed activity towards *cis*-Stilbene oxide (CSO), *trans*-Stilbene oxide (TSO) and 12(13) EpOME [12(13) epoxide of octadecamonoenoic acid/12(13) epoxide of linoleic acid] (Supplementary Fig. SF5) indicating its efficiency to utilize and hydrolyse aromatic and fatty acid epoxides. Biochemical characterization revealed stable activity of *Mi*EH2 between pH 7 to 8 with optima at pH 8 and > 40% reduction in activity below pH 6 and above pH 9. Activity profile of *Mi*EH2 at varied temperatures showed optima at 45 °C; while >40 reduction in the activity

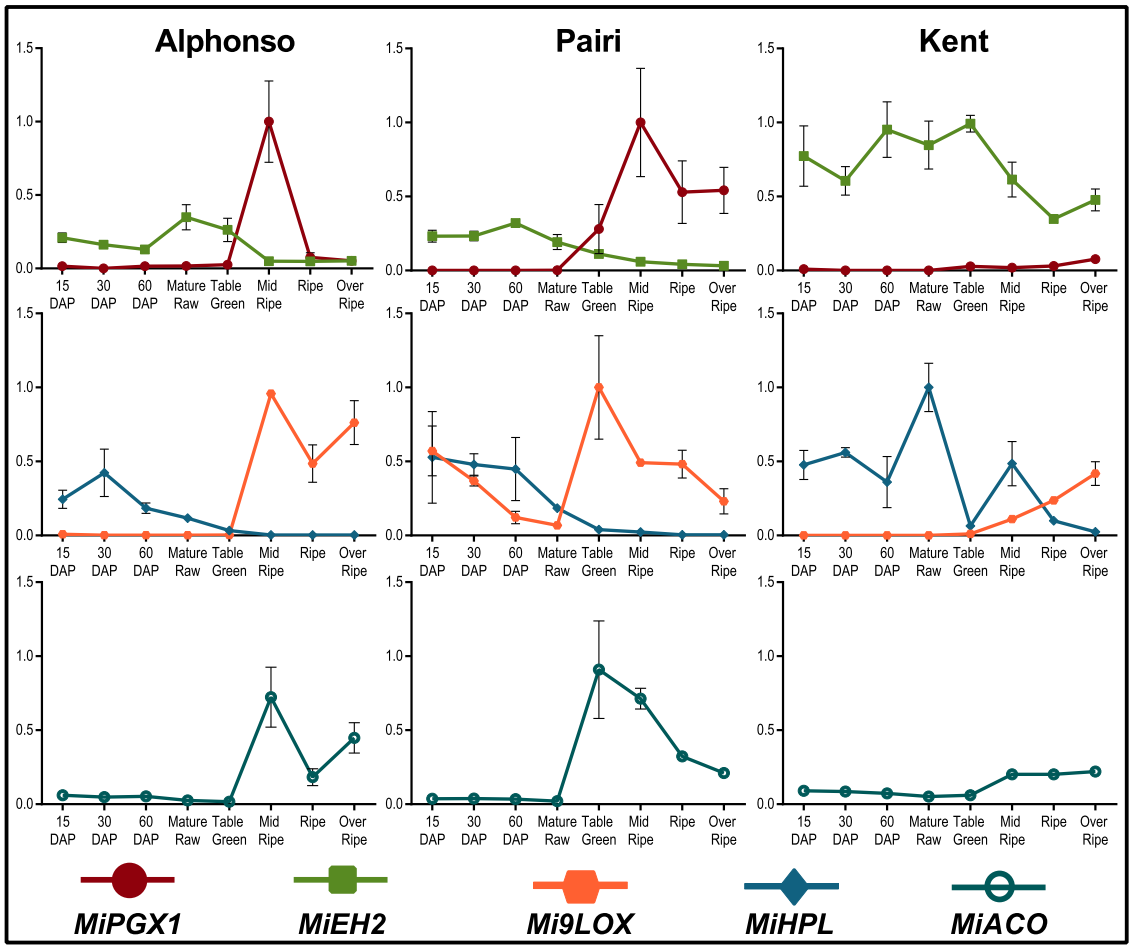

Fig. 3. Transcript profiles of *Mi9LOX*, *MiHPL*, *MiPGX1*, *MiEH2* and *MiACO* from skin tissue of various fruit development and ripening stages of Alphonso, Pairi and Kent mango cultivars. Vertical bars at each data point represent standard error in the relative quantification among the biological replicates. X axis represents fruit development and ripening stages and Y axis represents relative transcript abundance.

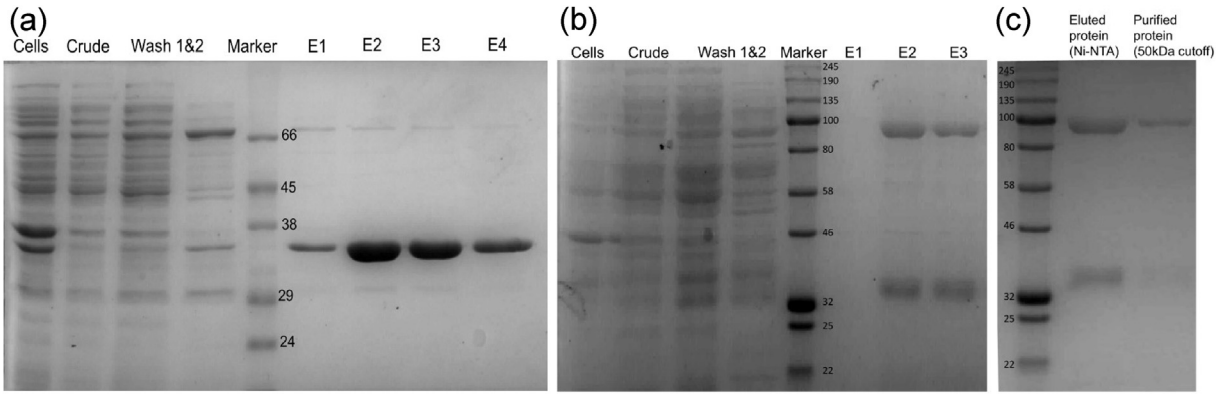

Fig. 4. CBB stained SDS-PAGE gels representing purified recombinant proteins *Mi*EH2 (a) and *Mi*9LOX (b) by Ni-NTA affinity purification and purified fraction of *Mi*9LOX after passing through 50 kDa cut-off column (c).

between 25 and 40 °C. Over 50% reduction in the activity was noted at 50 °C with complete inactivation at 60 °C and above (Supplementary Fig. Sf4). The *Mi*EH2 revealed higher Km and lower Vmax/Km value for CSO than TSO suggesting higher affinity and catalytic efficiency towards TSO (Table 1). Assay of *Mi*EH2 with 12(13) EpOME as substrate produced 12(13) DiHOME (12, 13 dihydroxy octadecamonoenoic acid) as a product (Supplementary Fig. SF5) confirming utilization of fatty acid epoxides as substrates. Vmax/Km value for 12(13) EpOME suggested its intermediate catalytic efficiency towards fatty acid substrates with respect to CSO and TSO (Table 1).

Table 1
Biochemical characterization and enzyme kinetics of recombinant *Mi*9LOX and *Mi*EH2.

Enzymes	*Mi*9LOX		*Mi*EH2		
Substrates	LA	ALA	CSO	TSO	12(13) EpOME
Vmax (μM min^{-1} mg^{-1})	611.11 ± 55.55	279.84 ± 5.87	26.53 ± 4.81	1055.55 ± 55.55	26.70 ± 0.04
Km (mM)	0.35 ± 0.03	0.06 ± $8E^{-5}$	0.17 ± 0.04	0.11 ± 0.003	0.004 ± 4.49 E^{-5}
Vmax/Km (min^{-1} mg^{-1})	1.73	4.56	0.16	9.34	6.19
Optimum temperature	37 °C	37 °C	45 °C	45 °C	–
Optimum pH	6.5	6.5	8	8	–

2.4. Transient over-expression of Mi9LOX and MiEH2 resulted in elevated lactone levels in mango fruit

Agrobacterium inoculation for test and control constructs was carried out in two halves of the same ethylene treated fruits as described (Supplementary Fig. SF6a), while Supplementary Fig. SF6b depicts a part of fruit checked by Gus staining to confirm expression of *GusA* along with the *Mi9LOX* or *MiEH2* after two days of *Agrobacterium* infiltration. The remaining tissue was used for the analysis of lactone content and gene expression to avoid error due to indigenous variation in lactone content and gene expression. *Mi9LOX* and *MiEH2* transcripts from test tissues upon *Agrobacterium* infiltration showed significant increase of 1.73 and 8.3-fold, respectively as compared to the control tissues (Fig. 5a). Intermediate metabolite analysis of these tissues by HRMS revealed significant increase of 1.9 folds in the 9HpOTrE upon *Mi9LOX* over-expression (Fig. 5b), whereas 9HpODE was not detected in the present analysis from control as well as test tissues. *MiEH2* over-expression resulted in the significant increase (2.57 folds) in the DHSA (DiHydroxy Stearic Acid) concentration (Fig. 5c). Another peak at mass 335.2, probably equivalent to exact mass of DiHODE (M^++Na^+) was also detected with significant increase (2.62 fold) in the test tissue as compared to the control. Volatile metabolite analysis by GC-MS of all these tissues indicated presence of eight lactones *viz.* γ-butyrolactone, δ-valerolactone, γ-hexalactone, δ-hexalactone, γ-octalactone, δ-octalactone, γ-decalactone and δ-decalactone while quantitative analysis by GC-FID showed increased levels of few lactones in both the sets (Fig. 5d and e). *Mi9LOX* transient over-expression resulted in significant increase at *p*-value ≤ 0.1 in the δ-valerolactone (0.075 μgg^{-1} to 0.082 μgg^{-1}) and δ-decalactone (0.043 μgg^{-1} to 0.064 μgg^{-1}) content (Fig. 5d). While *MiEH2* transient over-expression depicted significant

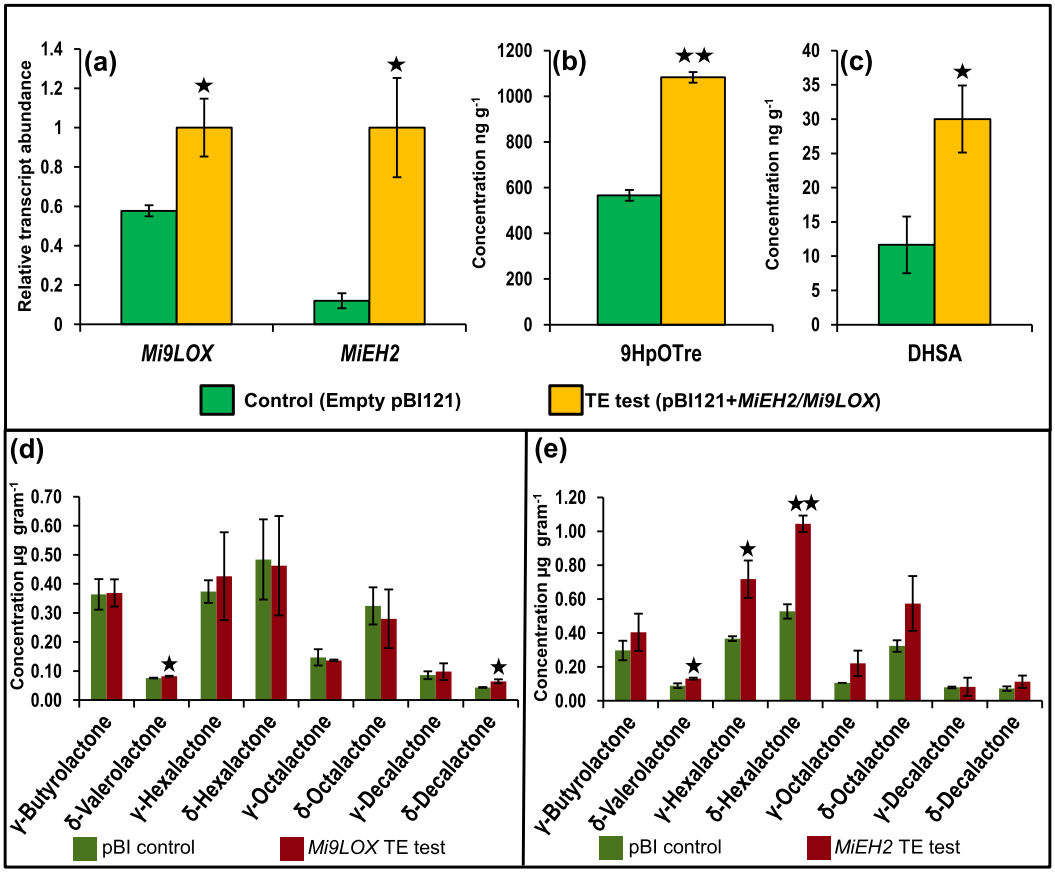

Fig. 5. Histogram representing changes in the *Mi9LOX* and *MiEH2* transcripts level in the control and test tissues after agroinfiltration (a). Histogram representing changes in the 9HpOTre (9-Hydroperoxy Octadeca Trienoic Acid) and DHSA (DiHydroxy Stearic Acid) content with respect to control upon transient over-expression of *Mi9LOX* (b) and *MiEH2* (c), respectively. Changes in the lactone content with respect to control upon transient over-expression of *Mi9LOX* (d) and *MiEH2* (e). Vertical bars represent standard error in the values from used data set, significance is represented as *- $p \leq 0.1$; **- $p \leq 0.05$.

increase at p-value $\leq$ 0.1 in δ-valerolactone (0.09 μgg^{-1} to 0.13 μgg^{-1}) and γ-hexalactone (0.37 μgg^{-1} to 0.72 μgg^{-1}) and highly significant increase at p-value $\leq$ 0.05 in δ-hexalactone (0.53 μgg^{-1} to 1.04 μgg^{-1}) compared to that in the control tissue (Fig. 5e).

3. Discussion

3.1. Mi9LOX and MiEH2 reveal catalytic properties similar to those of other plant 9LOX and EH2 enzymes

Lipoxygenase gene family, omnipresent to plant and animal kingdom comprises 9*LOX* and 13*LOX* as the most abundant classes (Feussner and Wasternack, 2002). The recombinant *Mi*9LOX protein characterized in the present study revealed optimum pH and temperature as well as thermal inactivation properties similar to that of other reported 9LOX enzymes (Baysal and Demirdöven, 2007; Huang and Schwab, 2011; Padilla et al., 2012; Santino et al., 2005). However, more affinity of *Mi*9LOX towards ALA than LA similar to that of olive 9LOX (Padilla et al., 2012) suggested probable tuning of this enzyme to *in vivo* availability of the substrate, as increased ALA content was observed during ripening of mango fruit (Deshpande et al., 2016).

Epoxide hydrolase genes fall into two classes *EH1* and *EH2*, which catalyse hydrolysis of aromatic epoxides and epoxides of fatty acids as well as aromatic compounds, respectively (Huang and Schwab, 2013; Wijekoon et al., 2008). The *Mi*EH2 in our study exhibited its promiscuous nature towards utilization of variety of substrates. It showed activity on CSO, TSO and 12(13) EpOME, however, more affinity towards TSO similar to EH2 reported from other plant species was observed (Bellevik et al., 2002a, 2002b; Huang and Schwab, 2013).

3.2. Role of Mi9LOX and MiEH2 in biosynthesis of lactones in Alphonso mango

The hydroperoxy and hydroxy fatty acids produced by *Mi*9LOX and *Mi*EH2 upon catalytic conversion of Δ9 unsaturated fatty acids (LA and ALA) and epoxy fatty acids, respectively are the potential precursors for lactone biosynthesis (Cardillo et al., 1989; Haffner and Tressl, 1998). We performed transient over-expression of *Mi9LOX* and *MiEH2* through *Agrobacterium* infiltration experiment to get insights into role of these genes in *de novo* biosynthesis of lactones in ripened mango fruits. Ethylene treated fruits were found to be ideal for transient expression to avoid the risk of bacterial and fungal infection owing to fruit injury during infiltration. Moreover, accelerated ripening and early appearance of lactones with no quantitative variation in Alphonso mango fruits upon exogenous ethylene treatment is known from our earlier studies (Chidley et al., 2013). Transient expression has been established as an efficient tool for functional characterization of genes (Orzaez et al., 2006; Spolaore et al., 2001) and clearly depicts its efficiency in the present study. Over-expression of *Mi9LOX* and *MiEH2* resulted in the significant increase in the content of their products 9HpOTrE and DHSA, respectively from the test tissue compared to the control. This confirms increased *Mi*9LOX and *Mi*EH2 enzyme activity in the tissue of transient over-expression of the respective genes; although the actual enzyme levels could not be assayed due to insufficient tissue availability. Further significant increase in the lactone content specifically δ-valerolactone (1.46 fold), γ-hexalactone (1.96 fold) and δ-hexalactone (1.98 fold) after *MiEH2* over-expression and, δ-valerolactone (1.08 fold) and δ-decalactone (1.48 fold) content upon *Mi9LOX* over-expression, respectively was evinced and confirms involvement of these genes in the lactone biosynthesis from mango fruit. Relatively less increase in δ-valerolactone content upon *Mi9LOX* over-expression might be because of less *Mi9LOX* transcripts post infiltration compared to *MiEH2* transcripts (Fig. 5a). Similarly, 9LOX is much upstream to the final product lactone and conversion of its products i.e. hydroperoxy fatty acids to hydroxy fatty acids by peroxygenase could be rate limiting.

3.3. Temporal expression of Mi9LOX, MiHPL, MiPGX1, MiEH2 and MiACO genes correlates with variable lactone content in fruit of mango cultivars

Lactone content varies amid the fruits of different mango cultivars (Pandit et al., 2009a). To get real insights of lactone biosynthesis in mango, three cultivars *viz.* Kent, Pairi and Alphonso with no, low (pulp, 1.3 μgg^{-1}; skin, 1.12 μgg^{-1}) and high (pulp, 7.12 μgg^{-1}; skin, 3.16 μgg^{-1}) lactone content, respectively were compared (Deshpande et al., 2016). In Alphonso pulp and skin tissues the highest transcript abundance of *Mi9LOX*, *MiPGX1* and *MiACO* was observed at mid ripe stage (10 DAH stage), which correlates with our earlier report of the first appearance of lactones at 10 DAH stage during Alphonso mango ripening (Kulkarni et al., 2012; Pandit et al., 2009b). In case of Pairi high abundance of *Mi9LOX* and *MiPGX1* transcripts detected at mid ripe stage but higher level of *MiACO* transcripts seen at table green stage (Figs. 2 and 3) indicates early onset of fatty acid degradation before the high abundance of *Mi9LOX* and *MiPGX1* transcripts. This probably makes reduced fatty acid substrate availability for lipoxygenase and peroxygenase resulting in low lactone content in Pairi fruits. Further significant reduction of *MiHPL* transcripts in these ripening tissues of Alphonso and Pairi suggests supply of hydroperoxy fatty acid pool to peroxygenase instead of HPL pathway. Previous studies on Alphonso have affirmed this by abundance of products of HPL pathway in the fruit developing stages than in the ripening stages (Pandit et al., 2009b). Contrary to this in Kent higher expression of *Mi9LOX*, *MiPGX1* and *MiACO* during the late ripening stages (ripe and over ripe stages) indicates delayed events for lactone biosynthesis (Figs. 2 and 3). Moreover, presence of *MiHPL* transcripts during fruit ripening signifies its co-expression with lipoxygenase diverting pool of hydroperoxy fatty acid to HPL pathway instead of peroxygenase pathway. This probably reasons the lactone less nature of Kent fruit.

Thus, altogether higher expression of *Mi9LOX*, *MiPGX1* and *MiACO* at mid ripe stage with adjournment of HPL pathway may result in high lactone content in Alphonso fruits. Early onset of fatty acid degradation may lead to low lactone content in Pairi. While delayed expression of *Mi9LOX*, *MiPGX1* and *MiACO* and depletion of hydroperoxy fatty acids by HPL pathway in combination with lower fatty acid content (Deshpande et al., 2016) may be the reason for no lactone content of Kent cultivar. In addition to this, variable *in vivo* conditions in the fruit of three cultivars might be responsible for differential catalytic efficiency of respective enzymes (though similar transcript abundance at respective maxima) leading to variation in lactone content. Further structural studies of these enzymes and *in vivo* substrate-product analysis using tracer technology might give better clarity about lactone biosynthesis in mango.

3.4. Proposed lactone biosynthesis pathway in mango

Based on our results and available information, we propose probable pathway of lactone biosynthesis in mango fruit (Fig. 6). *Mi*EH2 and *Mi*9LOX are part of monooxygenase (peroxygenase) and dioxygenase (lipoxygenase) pathways, respectively (steps A1 and B2; Fig. 6). Products of lipoxygenase are diverted to multiple pathways including hydroperoxide lyase (HPL) pathway (step C;

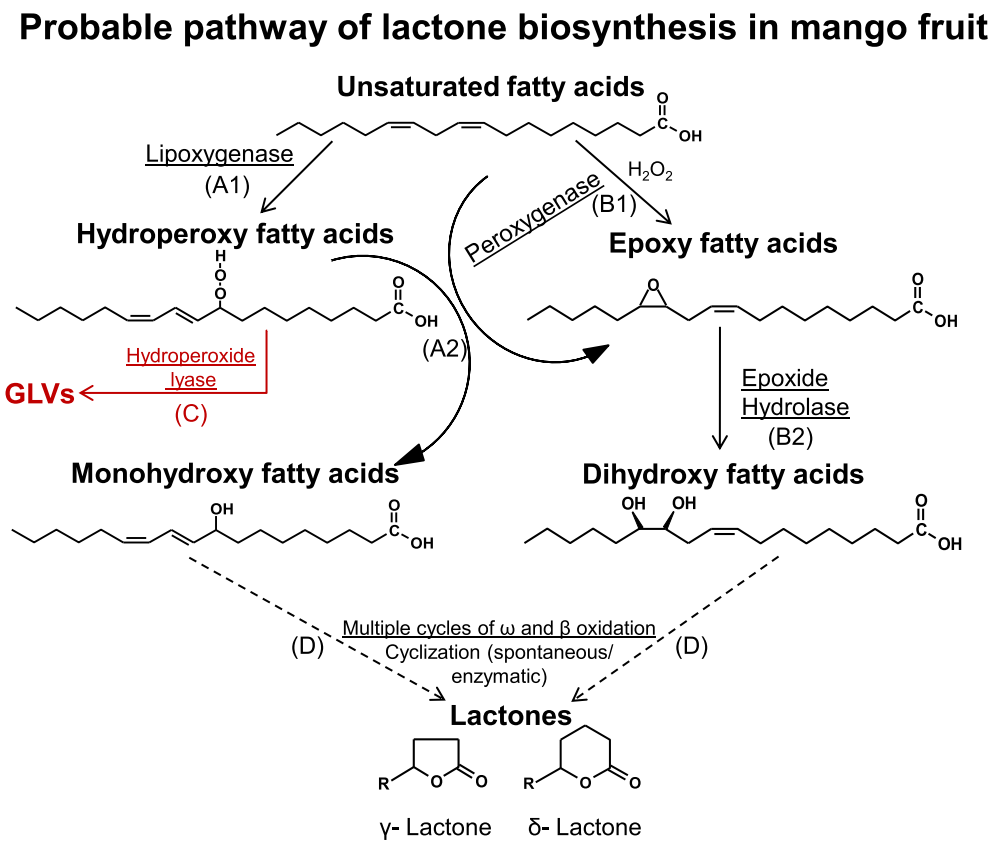

Fig. 6. Proposed pathway of lactone biosynthesis in mango fruit, words in bold represent metabolites; words underlined represent enzymes; A1, A2, B1, B2 and D steps are favourable for lactone biosynthesis. Step C; red in colour suggests unfavoured step for lactone biosynthesis. (For interpretation of the references to colour in this figure legend, the reader is referred to the web version of this article.)

Fig. 6), which produces C6 aldehydes and ketones responsible for fresh green leafy aroma volatiles (Huang and Schwab, 2011, 2012). This may divert hydroperoxy fatty acid pool to HPL pathway which is an unfavourable step for lactone biosynthesis. Products of lipoxygenase are also diverted to peroxygenase pathway. It is known that peroxygenase catalyzes epoxidation of unsaturated fatty acids using reactive oxygen (step B1; Fig. 6). Similarly it also utilizes hydroperoxy fatty acids as co-substrates or oxygen donor to produce epoxy and monohydroxy fatty acids (step A2; Fig. 6) (Babot et al., 2013; Fuchs and Schwab, 2013; Meesapyodsuk and Qiu, 2011). These epoxy fatty acids are further catalyzed by epoxide hydrolase to produce dihydroxy fatty acids (step B2; Fig. 6). In fungi the importance of fatty acid degradation in production of lactones from monohydroxy and dihydroxy fatty acids are well reported (Cardillo et al., 1989; Endrizzi et al., 1996; Haffner and Tressl, 1998; Schottler and Boland, 1996). Also in peach fruit post harvest temperatures influenced lactone content by regulation of *acyl-CoA-oxidase*, an important gene from β oxidation pathway of fatty acid degradation (step D; Fig. 6) (Xi et al., 2012). These findings insinuate that along with the *lipoxygenase* (*Mi9LOX*) and *epoxide hydrolase* (*MiEH2*), other genes *viz. peroxygenase* (*MiPGX1*), *hydroperoxide lyase* (*MiHPL*) and *acyl-CoA-oxidase* (*MiACO*) also play important role in lactone biosynthesis in mango (Fig. 6).

4. Conclusion

The genes encoding *Mi*9LOX, *Mi*EH2, *Mi*HPL, *Mi*PGX1 and *Mi*ACO were isolated from mango fruit. Variable lactone content of Alphonso, Pairi and Kent mango cultivars was elucidated by the expression analysis of these five genes during various fruit development and ripening stages of pulp and skin tissues of all the three cultivars. Among these *Mi*9LOX and *Mi*EH2 were characterized from Alphonso fruit, which divulged metabolism of unsaturated fatty acids leading to production of hydroperoxy fatty acid and hydroxy fatty acids, respectively. Increased lactone content upon transient over-expression of *Mi9LOX* and *MiEH2* ascertained their probable role in lactone biosynthesis in mango fruit. Finally, probable lactone biosynthetic pathway in mango was proposed.

5. Experimental

5.1. Plant material

Mangifera indica L. (Anacardiaceae) fruits of cv. Alphonso and cv. Pairi were collected from mango orchards at the Mango Research Sub Centre (16.528336 N, 73.344790 E), Deogad and of cv. Kent from mango orchards at the Regional Fruit Research Station (15.856849 N, 73.653387 E), Vengurle, both affiliated to Dr. Balasaheb Sawant Konkan Agricultural University, Dapoli, Maharashtra, India. Developing stages of all the three mango cultivars were collected at 15, 30 and 60 days after pollination (DAP) and at mature raw stage (90 DAP for cvs. Alphonso and Pairi, 110 DAP for cv. Kent). Fruits at these developing stages were harvested, pulp (mesocarp) and skin (exocarp) separated immediately, snap frozen in liquid nitrogen and stored at −80 °C until further use. A set of 12 fruits each for all the three cultivars were additionally harvested at their respective mature raw stage and kept in the hay containing boxes at ambient temperature for ripening. Three cultivars showed variation in the ripening duration, hence four ripening stages as table green, mid ripe, ripe and over ripe based on the skin colour, aroma and

fruit softness (each stage is represented by days after harvest i.e. DAH for cv. Alphonso as 5, 10, 15 and 20 days; for cv. Pairi as 4, 6, 8 and 10 days and for cv. Kent as 5, 8, 10 and 13 days, respectively) were used for further analysis. At each ripening stage fruits for each cultivar were removed from the box, pulp and skin were separated, frozen in liquid nitrogen and stored at −80 °C till further use. For transient expression studies ethylene treated fruits were collected as described earlier (Chidley et al., 2013).

5.2. RNA isolation and cDNA synthesis

Total RNA was isolated for all the tissues sampled for current study using RNeasy Plus mini kit (Quiagen, Venlo, The Netherlands). Two microgram of total RNA was reverse transcribed for synthesis of cDNA using High Capacity cDNA reverse transcription kit (Applied Biosystem, Carlsbad, CA, USA).

5.3. Isolation of open reading frames of Mi9LOX, MiHPL, MiPGX1, MiEH2 and MiACO

Full length gene sequences of *peroxygenase* (*PGX*), *hydroperoxide lyase (HPL) and acyl-CoA-oxidase (ACO)* were isolated from Alphonso mango using degenerate primers (Supplementary table ST1) approach. RACE reactions with gene specific primers (Supplementary table ST1) were carried out to obtain ends of *PGX, HPL* and *ACO* cDNAs. The terminal primers (Supplementary table ST1) were designed for each gene and the full-length genes were isolated and sequenced. These were blasted against the NCBI database for respective genes.

For isolation of partial gene sequence of *EH2* from Alphonso mango, degenerate primers *viz.* EH DeF1 and EH DeR4 (Supplementary table ST1) were designed by homology based approach aligning nucleotide sequences of *EH2* from other plant species available in NCBI database. Amplification was carried out using ripe stage cDNA as template. Amplicon with expected size was purified from agarose gel, cloned in pGEM-T easy vector (Promega, Madison, WI, USA) and sequenced to confirm partial cDNA sequence of *EH2*. Gene specific primers, EHRCF2 and EHRCR1 (Supplementary table ST1) were designed from the obtained sequence and used for rapid amplification of cDNA ends (RACE) to acquire the 5′ and 3′ ends using the SMART™ RACE cDNA Amplification Kit (Clontech, CA, USA). Those amplicons were cloned and sequenced to design terminal gene specific primers, EHtrF1and EHtrR1 (Supplementary table ST1) for the isolation of complete open reading frame (ORF) of *EH2*. For isolation of 9*LOX*, gene specific primers were designed from its available partial gene sequence (EU513272.1) from our previous study (Pandit et al., 2010). The same protocol as that of isolation of *EH2* ORF was further followed using LF1 and LR1 primers (Supplementary table ST1) to obtain cDNA ends and terminal primers LOX_TF1 and LOX_TR1 (Supplementary table ST1) to amplify complete ORF of 9*LOX*. Ripe mango cDNA as template and Advantage2 polymerase mix (Clontech) were used to get complete ORFs of both the genes (*MiEH2* and *Mi9LOX*) from mango, cloned in pGEM-T easy vector and transformed into *E. coli* (Top 10) cells. In both the cases presence of complete ORF was confirmed by sequencing plasmid inserts from number of positive colonies for each. Encoded proteins from these genes and other plant 9LOX, 13LOX, EH1 and EH2 from NCBI database were used for phylogenetic analysis. Neighbor joining tree was constructed by bootstrap test (1000 replicates) using MEGA 5.05.

5.4. Quantitative real-time PCR

Quantitative real-time PCR was performed using Fast Start Universal SYBR Green master mix (Roche Inc. Indianapolis, Indiana, USA) and *elongation factor 1α* (*EF1α*) as an endogenous control employing the primers reported earlier (Pandit et al., 2010). Transcripts of *Mi9LOX*, *MiEH2*, *MiPGX1*, *MiHPL and MiACO* were amplified using gene specific primers (Supplementary table ST1) and quantification was done by ViiA™ 7 Real-Time PCR System (Applied Biosystems) having thermal cycle program of initial denaturation at 95 °C for 10 min with subsequent 40 cycles of 95 °C for 3sec and 60 °C for 30 s followed by a dissociation curve analysis of transcripts. The analysis was carried out for pulp and skin tissues from all the developing and ripening stages of Alphonso, Pairi and Kent mango fruits.

Transcripts of *Mi9LOX* and *MiEH2* were also analysed in a similar way from the test and the control tissues obtained from transient over-expression experiments to understand changes in the transcript profiles upon *Agrobacterium* infiltration.

5.5. Cloning and recombinant expression of Mi9LOX and MiEH2 in E. coli

The full-length sequences of *Mi9LOX* and *MiEH2* amplified from the ripe Alphonso fruit cDNA using the Q5 High fidelity DNA polymerase (New England Biolabs Inc., Ipswich, MA, USA) and Advantage2 polymerase mix, respectively and the relevant terminal primers LOXpET101D F1/LOXpET101D R1 and EHTOPO_F1/EHTOPO_R1 (Supplementary table ST1) were cloned in the pET101D and pEXP5-CT/TOPO expression vectors (Invitrogen), respectively. After confirming the correct orientation of the insert and the presence of an uninterrupted reading frame by sequencing, the recombinant plasmids of *Mi*9LOX and *Mi*EH2 were transformed in the BL21(DE3) pLysS Rosetta cells (Novagen, Madison, WI, USA), for recombinant expression. Starter culture was initiated in 20 ml terrific broth (TB) with 100 $\mu g ml^{-1}$ ampicillin and grown at 37 °C with 180 rpm for 24 h. Expression culture was started with 1L TB medium inoculated with 1% final concentration of starter culture with 100 $\mu g ml^{-1}$ ampicillin at 37 °C with 180 rpm shaking speed. Expression of recombinant protein was induced by 0.2 mM IPTG at 0.6 OD_{600}. After induction expression culture was kept at 16 °C, 120 rpm for 12–14 h and cells were harvested by centrifugation, resuspended in100 mM phosphate buffer, pH 7 with 20 mM imidazole. The cells were lysed by sonication and the 6x-His tagged recombinant proteins were purified on Ni-NTA matrix (Invitrogen) wherein non-specifically bound proteins were removed by low molarity imidazole containing phosphate buffer washes. Recombinant proteins were eluted in 100 mM phosphate buffer with 250 mM imidazole (pH 7). In case of eluted *Mi*9LOX, low molecular weight contaminant proteins were removed by passing eluted fractions through Amicon Ultra centrifugal filters with NMWL 50 kDa membrane (Merck Millipore, Darmstadt, Germany). Purified recombinant proteins were checked by SDS-PAGE for their purity.

5.6. Enzyme assays of recombinant Mi9LOX and MiEH2

*Mi*9LOX activity assay was initially performed in 250 μl final volume of 100 mM phosphate citrate buffer, pH 7.0 containing 200 μM substrate i.e. linoleic acid (LA) or α-linolenic acid (ALA) and 0.005% Tween20 at 30 °C. The activity was measured by formation of the conjugated diene at 234 nm, applying an extinction coefficient 25,000 $M^{-1}cm^{-1}$ for both the substrates. A_{234} at 0^{th} min for each reaction was considered as blank and subtracted from A_{234} for given time (t). Similar activity assay was carried out for both the substrates with protein expressed from an empty vector. Optimum pH and temperature of the recombinant protein were determined by calculating *Mi*9LOX activity either at varied range of pH in

phosphate citrate buffer at 30 °C or in phosphate citrate buffer, pH 7 at various temperatures, respectively. After spectrophotometric measurement of catalytic activity of *Mi*9LOX, products were extracted in chloroform: methanol (2:1); completely dried in vacuum evaporator and reconstituted in methanol. These assay extracts were then used for UPLC coupled Q Exactive orbitrap HRMS (Thermo Scientific, Waltham, MA, USA) analysis for the product confirmation. Extracted compounds from the assay reactions were separated by water (A): methanol (B) solvent gradient, at 0 min with 70% (A)/30% (B); 0–2 min 50% (A)/50% (B); 2–12 min 0% (A)/100% (B), held for 2 min and again back to 70% (A)/30% (B) in 3 min with 2 min hold at flow rate 500 μl min^{-1}.

Recombinant *Mi*EH2 activity assay was carried out in 500 μl assay reaction in similar way as that of *Mi*9LOX using substrates *cis*-stilbene oxide (CSO), *trans*-stilbene oxide (TSO) and 12(13) epoxide of linoleic acid [12(13) EpOME]. Temperature and pH optimization was also carried out in a similar way. Products formed in the assay were extracted in chloroform: methanol (2:1); evaporated till dryness, reconstituted in 200 μl methanol and HRMS analysis was carried out by accurate mass (molecular ion) identification. Identified products from assay reaction were confirmed with the mass and retention time indices of authentic standards *R,R* hydrobenzoin and *meso* hydro benzoin. Extracted compounds from CSO and TSO assay reactions were separated by water (A): methanol (B) solvent gradient, 0–1 min with 80% (A)/20% (B); 1–2 min 60% (A)/40% (B); 2–4 min 40% (A)/60% (B); 4–11 min 20% (A)/80% (B); 11–16 min 0% (A)/100% (B), held for 2 min and again back to 80% (A)/20% (B) in 3 min with 2 min hold at flow rate 500 μl min^{-1}. Compounds from assay reactions of 12(13) EpOME were separated by using similar gradient program as that for *Mi*9LOX assay reaction. Graphs plotted with standard compounds were used for quantitative analysis of CSO and TSO products generated by recombinant *Mi*EH2. Full scans for both the programs were acquired on positive ion mode with AGC target value of 1E6, resolution of 70,000 at scan range 100–500 m/z, and maximum ion injection time (IT) of 250 ms.

5.7. Transient over-expression of Mi9LOX and MiEH2 in Alphonso mango fruits

The sequences of *Mi9LOX* and *MiEH2* were cloned separately at *Bam*HI restriction site in the pBI121 plant expression vector between CaMV 35S promoter and *GusA* gene using terminal primers (Supplementary table ST1). The resulted correctly oriented construct (A) pBI121 + *Mi9LOX*, construct (B) pBI121 + *MiEH2* and (C) pBI121 empty vector were transformed in *Agrobacterium tumefacience* GV3101 strain for transient expression studies. Separate *A. tumefacience* cultures (5 mL) were initiated for each construct from individual colonies in YEB medium (0.5% beef extract, 0.1% yeast extract, 0.5% peptone, 0.5% sucrose, 2 mM MgSO4) with 100 μgml^{-1} rifampicin and kanamycin antibiotics and incubated overnight at 28 °C. This culture was transferred to 50 mL induction medium, (YEB with 20 mM acetosyringone and 10 mM MES, pH 5.6) with 100 μgml^{-1} rifampicin and kanamycin antibiotics, and again grown overnight. Cultures were then recovered by centrifugation and re-suspended in infiltration medium (10 mM MgCl2, 10 mM MES, 200 mM acetosyringone, pH 5.6) till optical density reached to 1.0. This suspension was again incubated at 28 °C with gentle agitation for 2 h. Over-expression studies for *Mi9LOX* and *MiEH2* were carried out by *Agrobacterium* mediated infiltration in ethylene treated mango fruits at 3DAH stage by using hypodermic syringe. Equal volumes of (A) or (B) and (C) were used for infiltration in the two halves of the same mango fruit separated by fruit stone. During initial trials it was confirmed that, *Agrobacterium* mediated infiltration did not spread beyond fruit stone. Thus, control (C) and test (A/B) over-expressions were carried out in the same fruit. Five distinct mango fruits, each were used for the over-expression study of *Mi9LOX* and *MiEH2*. Infiltrated fruits were kept at 25 °C for 2 days in 12 h dark and light conditions each. After 2 days; a part from each of the fruit halves was checked by Gus staining (Kapila et al., 1997; Spolaore et al., 2001) to confirm expression of *Mi9LOX* and *MiEH2* each under 35S promoter along with *GusA* and remaining part of the fruit pulp was stored in −80 °C until used for the lactone analysis by gas chromatography.

5.8. Qualitative and quantitative analysis of metabolites

Aroma volatile extraction was carried out from 5 g of each tissue obtained from the transient over-expression experiment by solvent extraction method as mentioned earlier (Kulkarni et al., 2012; Pandit et al., 2009a). GC-MSD and GC-FID analysis for lactones was carried out on 7890B GC system Agilent Technologies coupled with Agilent 5977A MSD (Agilent technologies, Santa Clara, CA, USA). Aroma volatiles were separated on GsBP-5MS (General Separation Technologies, Newark, DE) capillary column (30 m × 0.32 mm i.d. × 0.25 μm film thickness). Other chromatographic conditions were maintained as reported earlier (Kulkarni et al., 2012). To understand the effect of transient over-expression of *Mi9LOX* and *MiEH2* on lactone biosynthesis, qualitative and quantitative analysis of lactones alone was carried out in the present study. Lactones were identified by matching generated spectra with NIST 2011 and Wiley 10th edition mass spectral libraries. Identified compounds were confirmed by matching retention time and spectra of authentic standards procured from Sigma Aldrich (St. Louis, MO, USA). Absolute quantification was done using nonyl acetate as internal standard and by normalizing concentration of all the individual lactones with that of known concentration of internal standard.

Qualitative and quantitative analysis of *Mi*9LOX and *Mi*EH2 products from tissues obtained after transient over-expression was carried out on UPLC coupled Q-Exactive orbitrap HRMS (Thermo Scientific, Waltham, MA, USA) in a similar way done for the *Mi*9LOX and *Mi*EH2 assay products. Extraction of these intermediate compounds was carried out from 0.5 g tissue obtained from the transient over-expression experiment.Tissue was grinded in liquid nitrogen and added to 2 ml of 80% methanol, vortexed and sonicated for 5 min and fatty acid intermediates were extracted in 1 ml of hexane. Hexane layer was removed and evaporated to complete dryness and metabolites were reconstituted in 100 μl of 100% methanol and further used for HRMS analysis.

5.9. Statistical analysis

Experiments for each developing and ripening stages were performed from fruits of 3 independent trees for cv. Alphonso and 2 independent trees each for cv. Pairi and cv. Kent. These were considered as biological replicates. Extraction of volatiles in transient over-expression studies was carried out twice for each tissue as technical replicates followed by duplicate GC-FID runs of each extract as analytical replicates. Quantitative real time PCR analysis was carried out in triplicate for each biological replicate from Alphonso, Pairi and Kent cultivars. Fisher's LSD test was performed at $p \leq 0.05$ and $p \leq 0.1$ by ANOVA for comparative analysis of lactone content in control and test tissues in transient expression analysis using Stat View software, version 5.0 (SAS Institute Inc., Cary, NC, USA). Similarly ANOVA was carried out for comparison of *Mi9LOX, MiEH2, MiPGX1, MiHPL and MiACO* transcripts at various fruit development and ripening stages from pulp and skin tissues of Alphonso, Pairi and Kent cultivars.

Authors' contributions

ABD designed, standardized and performed majority of the experiments, analysed the data and wrote the manuscript. HGC carried out isolation of complete ORF of HPL and partial cds of 9*LOX*. PSO helped with RNA isolation, cDNA synthesis and qPCR studies. KHP contributed by providing the experimental tissue. APG contributed with suggestions for the work and for manuscript planning. VSG designed the study, participated in all parts of the work and contributed to the preparation of the manuscript. All authors read and approved the final manuscript.

Conflict of interest

Provisional patent applications related to this manuscript with the "Organization as applicant" and "Authors as inventors" have been filed with application numbers 201611011374 and 201611011975. No other competing interests exist.

Acknowledgements

A.B.D, H.G.C. and P.S.O. thank CSIR and UGC for research fellowships. Dr. Balasaheb Sawant Konkan Agriculture University staff and Mr. Kiran Malshe are acknowledged for their field support at Deogad and Vengurle Research Stations. Support from Dr. Mahesh Kulkarni and Ms. Gouri Patil, CSIR-National Chemical Laboratory, Pune for spectrophotometric analysis is thankfully acknowledged. Authors also thank Mr. Rahul Tanpure for his help to carry out *Agrobacterium* mediated infiltration experiments. This research was funded by the Council of Scientific and Industrial Research, New Delhi, India under project CSC0133 (FUNHEALTH) to CSIR-NCL and 21(0997)/16/EMR-II grant as Emeritus Scientist scheme to Dr. Vidya Gupta.

Appendix A. Supplementary data

Supplementary data related to this article can be found at http://dx.doi.org/10.1016/j.phytochem.2017.03.002.

References

Babot, E.D., del Rio, J.C., Kalum, L., Martinez, A.T., Gutierrez, A., 2013. Oxyfunctionalization of aliphatic compounds by a recombinant peroxygenase from *Coprinopsis cinerea*. Biotechnol. Bioeng. 110, 2323–2332.

Baysal, T., Demirdöven, A., 2007. Lipoxygenase in fruits and vegetables: a review. Enzyme Microb. Technol. 40, 491–496.

Bellevik, S., Summerer, S., Meijer, J., 2002a. Overexpression of *Arabidopsis thaliana* soluble epoxide hydrolase 1 in *Pichia pastoris* and characterisation of the recombinant enzyme. Protein Expr. Purif. 26, 65–70.

Bellevik, S., Zhang, J.M., Meijer, J., 2002b. *Brassica napus* soluble epoxide hydrolase (BNSEH1) - cloning and characterization of the recombinant enzyme expressed in *Pichia pastoris*. Eur. J. Biochem. 269, 5295–5302.

Cardillo, R., Fronza, G., Fuganti, C., Grasselli, P., Nepoti, V., Barbeni, M., Guarda, P.A., 1989. On the mode of conversion of racemic, c14-c19, gamma-hydroxy alkene fatty-acids into c7-c11, optically-active gamma-lactones and delta-lactones in *Cladosporium suaveolens*. J. Org. Chem. 54, 4979–4980.

Chidley, H.G., Kulkarni, R.S., Pujari, K.H., Giri, A.P., Gupta, V.S., 2013. Spatial and temporal changes in the volatile profile of Alphonso mango upon exogenous ethylene treatment. Food Chem. 136, 585–594.

Dar, S.M., Oak, P., Chidley, H., Deshpande, A., Giri, A., Gupta, V., 2016. Chapter 19-nutrient and flavor content of mango (*Mangifera indica* L.) cultivars: an appurtenance to the list of staple foods A2-preedy. In: Monique, S.J., SimmondsVictor, R. (Eds.), Nutritional Composition of Fruit Cultivars. Academic Press, San Diego, pp. 445–467.

Deshpande, A.B., Chidley, H.G., Oak, P.S., Pujari, K.H., Giri, A.P., Gupta, V.S., 2016. Data on changes in the fatty acid composition during fruit development and ripening of three mango cultivars (Alphonso, Pairi and Kent) varying in lactone content. Data Brief 9, 480–491.

Endrizzi, A., Pagot, Y., LeClainche, A., Nicaud, J.M., Belin, J.M., 1996. Production of lactones and peroxisomal beta-oxidation in yeasts. Crit. Rev. Biotechnol. 16, 301–329.

Feussner, I., Wasternack, C., 2002. The lipoxygenase pathway. Annu. Rev. Plant Biol. 2002 (53), 275–297.

Fuchs, C., Schwab, W., 2013. Epoxidation, hydroxylation and aromatization is catalyzed by a peroxygenase from *Solanum lycopersicum*. J. Mol. Catal. B Enzymatic 96, 52–60.

Haffner, T., Nordsieck, A., Tressl, R., 1996. Biosynthesis of delta-Jasmin lactone(=(Z)-Dec-7-eno-5-lactone) and (Z,Z)-Dodeca-6,9-dieno-4-lactone in the yeast *Sporobolomyces odorus*. Helvetica Chim. Acta 79, 2088–2099.

Haffner, T., Tressl, R., 1998. Stereospecific metabolism of isomeric epoxyoctadecanoic acids in the lactone-producing yeast *Sporidiobolus salmonicolor*. Lipids 33, 47–58.

Huang, F.-C., Schwab, W., 2011. Cloning and characterization of a 9-lipoxygenase gene induced by pathogen attack from *Nicotiana benthamiana* for biotechnological application. BMC Biotechnol. 11.

Huang, F.-C., Schwab, W., 2012. Overexpression of hydroperoxide lyase, peroxygenase and epoxide hydrolase in tobacco for the biotechnological production of flavours and polymer precursors. Plant Biotechnol. J. 10, 1099–1109.

Huang, F.-C., Schwab, W., 2013. Molecular characterization of NbEH1 and NbEH2, two epoxide hydrolases from *Nicotiana benthamiana*. Phytochemistry 90, 6–15.

Idstein, H., Schreier, P., 1985. Volatile constituents of alphonso mango (*Mangifera indica*). Phytochemistry 24, 2313–2316.

Kapila, J., DeRycke, R., VanMontagu, M., Angenon, G., 1997. An Agrobacterium-mediated transient gene expression system for intact leaves. Plant Sci. 122, 101–108.

Kulkarni, R.S., Chidley, H.G., Pujari, K.H., Giri, A.P., Gupta, V.S., 2012. Geographic variation in the flavour volatiles of Alphonso mango. Food Chem. 130, 58–66.

Meesapyodsuk, D., Qiu, X., 2011. A peroxygenase pathway involved in the biosynthesis of epoxy fatty acids in oat. Plant Physiol. 157, 454–463.

Muys, T.G., Jonge, A.P.D., Vanderven, B., 1962. Synthesis of optically active gamma- and delta-lactones by microbiological reduction. Nature 194, 995–996.

Orzaez, D., Mirabel, S., Wieland, W.H., Granell, A., 2006. Agroinjection of tomato fruits. A tool for rapid functional analysis of transgenes directly in fruit. Plant Physiol. 140, 3–11.

Padilla, M.N., Luisa Hernandez, M., Sanz, C., Martinez-Rivas, J.M., 2012. Molecular cloning, functional characterization and transcriptional regulation of a 9-lipoxygenase gene from olive. Phytochemistry 74, 58–68.

Pandit, S.S., Chidley, H.G., Kulkarni, R.S., Pujari, K.H., Giri, A.P., Gupta, V.S., 2009a. Cultivar relationships in mango based on fruit volatile profiles. Food Chem. 114, 363–372.

Pandit, S.S., Kulkarni, R.S., Chidley, H.G., Giri, A.P., Pujari, K.H., Kollner, T.G., Degenhardt, J., Gershenzon, J., Gupta, V.S., 2009b. Changes in volatile composition during fruit development and ripening of 'Alphonso' mango. J. Sci. Food Agric. 89, 2071–2081.

Pandit, S.S., Kulkarni, R.S., Giri, A.P., Koellner, T.G., Degenhardt, J., Gershenzon, J., Gupta, V.S., 2010. Expression profiling of various genes during the fruit development and ripening of mango. Plant Physiol. Biochem. 48, 426–433.

Santino, A., Iannacone, R., Hughes, R., Casey, R., Mita, G., 2005. Cloning and characterisation of an almond 9-lipoxygenase expressed early during seed development. Plant Sci. 168, 699–706.

Schottler, M., Boland, W., 1996. Biosynthesis of dodecano-4-lactone in ripening fruits: crucial role of an epoxide-hydrolase in enantioselective generation of aroma components of the nectarine (*Prunus persica* var Nucipersica) and the strawberry (*Fragaria ananassa*). Helvetica Chim. Acta 79, 1488–1496.

Spolaore, S., Trainotti, L., Casadoro, G., 2001. A simple protocol for transient gene expression in ripe fleshy fruit mediated by *Agrobacterium*. J. Exp. Bot. 52, 845–850.

Vecchietti, A., Lazzari, B., Ortugno, C., Bianchi, F., Malinverni, R., Caprera, A., Mignani, I., Pozzi, C., 2009. Comparative analysis of expressed sequence tags from tissues in ripening stages of peach (*Prunus persica* L. Batsch). Tree Genet. Genomes 5, 377–391.

Wijekoon, C.P., Goodwin, P.H., Hsiang, T., 2008. The involvement of two epoxide hydrolase genes, NbEH1.1 and NbEH1.2, of *Nicotiana benthamiana* in the interaction with *Colletotrichum destructivum, Colletotrichum orbiculare* or *Pseudomonas syringae* pv. tabaci. Funct. Plant Biol. 35, 1112–1122.

Wilson, C.W., Shaw, P.E., Knight, R.J., 1990. Importance of some lactones and 2,5-dimethyl-4-hydroxy-3(2h)-furanone to mango (*Mangifera indica* L.) aroma. J. Agric. Food Chem. 38, 1556–1559.

Xi, W.-P., Zhang, B., Liang, L., Shen, J.-Y., Wei, W.-W., Xu, C.-J., Allan, A.C., Ferguson, I.B., Chen, K.-S., 2012. Postharvest temperature influences volatile lactone production via regulation of acyl-CoA oxidases in peach fruit. Plant Cell Environ. 35, 534–545.